International Journal of Technology

http://ijtech.eng.ui.ac.id

Research Article

Preparation and Characterization of Activated Carbon from Cavendish Banana (*Musa acuminata*) Peels for Ferric Ions Adsorption

Restu Kartiko Widi [1], Puguh Setyopratomo [1], Priscilla Eveline Danatha [1], Verina Dione Nanlohy [1], Emma Savitri [1,*]

[1]*Chemical Engineering Department, Engineering Faculty, University of Surabaya Raya Kalirungkut Tenggilis, Surabaya, East Java, Indonesia 60290*
[*]*Corresponding author: savitri_ma@staff.ubaya.ac.id; Tel.: +62 81331766758*

Abstract: This research aimed to investigate the effect of carbonization temperature, type, and acid concentration as an activating agent on the physicochemical properties of activated carbon made from banana (Musa acuminata) peels waste. Carbonization was performed at four different temperatures of 200, 300, 400, and 500°C for two hours, while chemical activation was carried out using varying concentrations of hydrochloric and phosphoric acid. During the experiment, carbon was impregnated with HCl and H_3PO_4 at three varying solution concentrations of 3, 6, and 9 % for 24 hours. Subsequently, sample characterization was conducted using ASTM D2867, ASTM D2866, ASTM D4607, morphology was observed with SEM, the functional group was analyzed using FT-IR, and BET equipment was applied to determine physicochemical properties. Activated carbon was used as an adsorbent to remove ferric ions and iodine (I_2) from the solution. The results showed that the product derived from carbonization at 300°C and activation using 9% hydrochloric acid produced the highest adsorption capacity of 1.104 mg/g and 1881.51mg/g for ferric ions and iodine, respectively. Moreover, activated carbon derived from banana peels showed the potential to be regenerated for approximately four times, but with a decrease in efficiency to 75%.

Keywords: Acid activation; Activated carbon; Banana peels; Carbonization; Ferric ions adsorption

1. Introduction

The rapid growth in population and urbanization in the last few decades is associated with an increase in water scarcity and low quality. To overcome several water supply quality problems, various conventional treatment methods have been used, including disinfection, desalination, and decontamination. However, these methods cannot be widely applied due to the expensive costs and production of residues, which contributes to freshwater contamination (Adekanmi, 2021), showing the need to develop new strategies. In this context, adsorption has been proven as a promising technology due to the simple infrastructure, improved efficiency, and effectiveness. Several different adsorbents have also been reported for the treatment of polluted water (Dhaneswara et al., 2024; Darmadi et al., 2023; Timotius et al., 2022; Basuki et al., 2021; Kusrini et al., 2021).

This work was supported by the Indonesian Ministry of Research, Technology, and Higher Education funded by Fundamental Research and number 077/E5/PG.02.00.PL/2023 and 004/SP2H/PT-L/LL7/2023

https://doi.org/10.14716/ijtech.v16i4.6664
Received September 2023; Revised February 2024; Accepted April 2024

Among the existing adsorbents, activated carbon is considered effective for solving various water problems such as taste, odor, and the removal of unwanted contaminants including heavy metals, chlorine, and volatile organic compounds (VOCs)(Basheer et al., 2021; Peláez-Cid et al., 2020; Sanchez-Sanchez et al., 2020; Yu et al., 2020; Zhang et al., 2019). Activated carbon is a material with a very high surface area, which is prepared using both physical and chemical methods. Physical treatment consists of a two-step process comprising carbonization, followed by gasification of oxidizing agents usually CO_2 and water vapor. Meanwhile, chemical treatment is a one-step process where carbonization and activation occur simultaneously, using compounds such as $ZnCl_2$, H_3PO_4, KOH, and NaOH (Wang and Xu, 2024; Mistar et al., 2020; ElShafei et al., 2014). The high cost of production has been the most challenging part of commercially producing activated carbon. This has led to the exploration of inexpensive raw materials with high carbon, low inorganic content workability, minimum impact on the environment, and storage life, as desirable precursors in recent decades. Moreover, both physical and chemical treatments can produce a very high specific surface area of activated carbon. Renewable sources are the most widely used materials due to the exceptional adsorbent properties (Bhushan et al., 2021; Prakash et al., 2021; Yağmur and Kaya, 2021).

Banana is a widespread fruit available globally, including in Indonesia, where peels are easily accessible to make activated carbon without significant cost. This application is widely accepted due to several factors such as the high content of fiber and organic compounds, namely cellulose, lignin, and pectin. The fiber contributes to the formation of a strong structure and large pores in activated carbon. Additionally, the organic components produce activated carbon with various pores, including micro- and meso-, which is essential as an adsorbent for both organic and inorganic pollutants. Another advantage is that banana peels waste decomposes naturally, rendering the use as activated carbon environmentally friendly, presenting the material as an attractive option for the manufacturing process (Yanti et al., 2023; Wikantika et al., 2022; Jodiawan et al., 2021; Falowo et al., 2021; Tripathy et al., 2021; Anhwange et al., 2009). In this research, Cavendish banana peels waste (*Musa acuminata*) was used to produce activated carbon based on the high organic carbon content, such as lignocellulose, reaching 97.5% compared to other types, namely Saba (*Musa paradisiaca var. sapientum*) or King banana (*Musa paradisiaca*) which ranged from 90 to 92% (Anhwange et al., 2009). The conversion of banana peels waste into activated carbon is aimed at increasing the economic value, reducing waste disposal costs, and providing inexpensive raw materials. Although previous investigation (Din et al., 2017) used acid impregnation process before carbonization, this research applied carbonization process at the initial stage to form more and stronger activated carbon pores before being activated using acid solution to obtain greater adsorption capacity. Initially, banana peels waste was dried, carbonized, and activated using acid solution. The product obtained was tested for the performance as an adsorbent to remove ferric ions in solution.

2. Method

Activated carbon was prepared according to the method of (Din et al., 2017), but conducted in the reverse order. This method was used to control the structure and pore size, producing activated carbon with high adsorption capacity for specific molecules. The production of activated carbon from Cavendish banana peels consisted of three stages. Initially, sample preparation and dehydration processes were carried out, followed by carbonization and chemical activation. Activated carbon produced at optimum conditions was used as an adsorbent to adsorb ferric ions from the solution, followed by the analysis of adsorption capacity and model.

2.1. Sample Preparation

In this experiment, cavendish banana peels were used as raw materials for producing activated carbon. The starting materials were cut into a size of 2 x 2 cm^2 and dried in an oven at 110°C for 1 hour. The dried samples were prepared by carbonization and chemical activation. The carbonization process was carried out at 200, 300, 400, and 500°C for 2 hours. Subsequently,

carbonized samples were crushed and activated in a 3-9 % (by volume ratio) H_3PO_4 and HCl solution for 24 hours. The slurry was placed into a separating funnel to recover the solid part as activated carbon from the liquid. The sample was washed successively with distilled water and dried at 105°C for 30 minutes to obtain activated carbon. This was followed by the analysis of moisture, ash content, and absorption capacity for iodine and ferric ions solutions. The schematic diagram for the production process is shown in Figure 1.

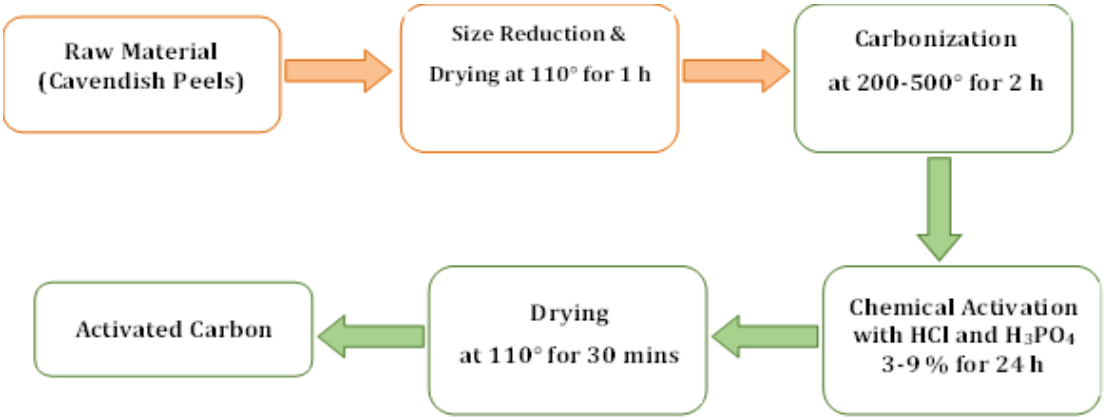

Figure 1 Schematic Diagram for Producing Activated Carbon from Cavendish Banana Peels

2.2. Characterization of Activated Carbon

Activated carbon samples were characterized using ASTM D2867, D2866, and D4607 standards, including moisture and ash content analysis, as well as iodine adsorption. Characterization was carried out to measure the quality of activated carbon produced in several different process conditions.

Table 1 Activated carbon quality based on ASTM D2867, D2866, and D4607 standards

Parameter	Unit	Requirement
Moisture content	%	≤ 5-10
Ash content	%	≤ 5-8
Iodine adsorption	mg/g	≥ 500

Moisture contents were measured by weighing 1 g of activated carbon, and heating at 105°C for 6 hours, followed by weight measurement. Moisture content was defined as equation 1.

$$\text{Moisture content (\%)} = \frac{Samples\ mass\ difference}{Initial\ samples\ mass\ before\ heating}\ 100\% \quad (1)$$

Ash contents were measured by combusting 1 g of raw materials in a muffle furnace at 650°C for 4 hours, followed by weighing activated carbon after heating. Ash content was defined as equation 2

$$\text{Ash content (\%)} = \frac{Total\ ash\ mass}{Initial\ samples\ mass}\ x\ 100\% \quad (2)$$

The iodine number was obtained based on the ASTM D4607 standard test method by incorporating 0.5 g of activated carbon into Erlenmeyer containing 25 mL of 0.1 N iodine solution and shaking gently for 15 minutes. The solution was filtered and the filtrate obtained was placed into an Erlenmeyer for titration using 0.1 N sodium thiosulphate ($Na_2S_2O_3$) solution until it turned yellowish. Approximately 1 mL of 1% starch solution was added to the solution, and the titration was continued to obtain a clear solution. The concentration of iodine solution was calculated from a total volume of $Na_2S_2O_3$ used and the volume dilution factor (see equation 3)

$$I = \frac{(V_1N_1 - V_2N_2)x\ Mr\ Iodine\ x\ f_D}{Activated\ carbon\ mass} \quad (3)$$

where I is Iodine adsorption (mg/g), V_1 is iodine solution volume (mL), N_1 is iodine concentration (N), V_2 is sodium thiosulphate solution volume used (mL), N_2 is sodium thiosulphate concentration (N), Mr is molecular weight (g/mol), and f_D is dilution factor.

The morphological properties of activated carbon were analyzed by Scanning Electron Microscopy (SEM). A scanning electron microscope (SEM FEI INSPECT S-50, Netherlands) was used to determine the morphology of the sample. Subsequently, activated carbon was sprinkled on double-sided carbon tape, placed on the sample holder, and coated with gold.

The FT-IR analysis is used to identify the functional groups in activated carbon. These groups are important for heavy metal adsorption and determine the type of adsorption process. Subsequently, FT-IR spectroscopy (FT-IR Shimadzu IR Tracer 100, Japan) was applied to observe functional group changes before and after carbonization using the KBr disc method. Activated carbon was mixed with dry KBr (ratio of 1:100) and pressed into a transparent disc. FTIR spectroscopy was conducted for the range of 4000 – 400 cm^{-1}. All of the spectra were recorded at room temperature with a resolution of 4 cm^{-1} and 45 scans.

The surface area of samples was determined using Brunauer-Emmett-Teller (BET) nitrogen adsorption-desorption measurements at 77 K. The Micromeritics Gemini VII Version 5.03 equipment was used to determine the surface area and pore size characteristics through volumetric adsorption of N2 at 77 K. Activated carbon was degasified at 300°C for one hour to eliminate any adsorbed species. Subsequently, the nitrogen adsorption at a relative pressure of 0.99 was used to determine the total pore volume.

2.3. Adsorption Model of Ferric ions with Activated Carbon

The solutions of ferric ions solution were mixed with activated carbon and stirred at room temperature using batch experiment. Subsequently, the solutions were filtered, and the concentrations of ferric ions were determined using Genesys 150 UV-Visible Spectrophotometer (Thermo Scientific, USA) at 510 nm. The equilibrium concentrations of the adsorbates in the solid phase relative to the concentrations in the liquid phase (Q_e, mg/g) of activated carbon were determined based on adsorbate mass balance using equation (4) (Zhou et al., 2023) :

$$Q_e = \frac{(C_0 - C_e) x\, V}{M} \tag{4}$$

where Co and Ce are the initial and equilibrium ferric ions concentrations (mg/L), respectively, V is the volume of the aqueous solution (L), and M is the mass of activated carbon used (g).

Adsorption is a mass transfer process that occurs when materials accumulate at the interface between solid and liquid phases. This process is described by equilibrium relationships between sorbent and sorption isotherms, which typically represent the ratio of the quantity of sorbed material to the remaining material in the solution at a fixed temperature and in a state of equilibrium. The adsorption behaviour of activated carbon from Cavendish banana peels waste for ferric ions solution could be elucidated by adsorption models. Several theories have been applied to describe adsorption equilibrium, with numerous isotherm equations available. However, this research focuses on two key isotherms, namely the Langmuir and Freundlich. The equations for these models are stated as follows (Zhou et al., 2023).

$$\frac{C_e}{Q_e} = \frac{C_e}{Q_m} + \frac{1}{K_L Q_m}\ (Langmuir) \tag{5}$$

$$ln\, Q_e = ln\, K_f + \frac{1}{n} ln\, C_e\ (Freundlich) \tag{6}$$

where Q_e, C_0, and C_e are the same as in Equation (4). Q_m is the maximum theoretical adsorption capacity of activated carbon for ferric ions. K_L and K_F are the adsorption constants of the Langmuir and Freundlich isotherm models related to the adsorption capacity, respectively. 1/n is the constant of adsorption intensity or the surface heterogeneity.

3. Results and Discussion

3.1. Carbonization of Cavendish Banana Peels Waste

Carbonization is an incomplete combustion process of organic material due to limited air availability leading to decomposition. This process is carried out to produce granular carbon with a neat structure, significantly increasing the adsorption ability. In this research, a significant decrease in the component of the organic material was observed to occur at 400°C due to the decomposition of lignocellulosic biomass, including hemicellulose, cellulose, and lignin. Based on the results, lignin was the first component to decompose at low temperatures and continued until 900°C. At approximately 200°C, carbonization produced a product similar to biochar and pure carbon. Hemicellulose decomposed at low temperatures between 200 and 360°C, while cellulose decomposed at the high-temperature range of 240-390°C. At 300-400°C temperature, carbonization tended to produce carbon products with some organic contaminations. Moreover, at temperatures above 400°C, the final decomposition of the aromatic lignin fraction occurred, producing carbon purer than the product from the carbonization process at 300-400°C with insignificant organic contamination (Luangkiattikhun et al., 2008). The characteristics of carbon produced from the carbonization process at different temperatures are shown in Table 2.

Table 2 shows that the moisture content obtained from carbonization process at various temperatures ranged from 28.75 to 30.82%. The lowest moisture content of 28.75% occurred at carbonization temperature of 300°C. Based on the results, an increase in the temperature caused a high decomposition of all organic components, leading to the production of carbon with more pores and a regular shape. Additionally, high temperature caused an increase in moisture equilibrium of carbon material with the environment. The highest moisture content was obtained at carbonization temperature of 500°C.

Table 2 Carbon characterization after carbonization at different temperatures

Carbonization Temperature, °C	Parameters		
	Moisture Content, %	Ash Content, %	Iodine Adsorption, mg/g
200	30.51	1.80	1845.03
300	28.75	1.32	1881.51
400	29.81	3.22	1855.29
500	30.82	5.57	1728.10

Carbonization at 200°C produced carbon with a higher moisture content than at 300°C. This was because most of the lignocellulose, namely hemicellulose and cellulose had not been decomposed at 200°C. Therefore, carbon produced had various organic contents, causing an increase in moisture content. Table 2 shows that carbon ash content was in the range of 1.80 – 5.57%. Ash is produced from the combustion of organic materials containing mineral and inorganic compounds. Moreover, a high ash content of carbonized carbon contributes to a reduction in performance due to the potential blockages in the pores and decreased adsorption capability (Tongpoothorn et al., 2011; Sudaryanto et al., 2006). Previous research reported that higher carbonization temperature produced greater ash content value of activated carbon (Hendrawan et al., 2017). Based on the results, there was an increase in iodine absorption from carbonization at 300˚C due to higher carbon yield and increased pore volume. The pores formed were also more regular, leading to a larger surface area of carbon material (Hendrawan et al., 2017). The increased number of pores and carbon surface area enhanced absorption capacity, thereby improving iodine adsorption. However, carbonization at 400 and 500˚C decreased the absorption capacity for iodine due to the higher amount of moisture and ash content produced compared to carbonization temperature of 300˚C. The high ash content led to blockage of carbon pores and affected iodine adsorption capacity. Additionally, the high moisture content caused carbon sites to be filled with water molecules, preventing the adsorption of iodine.

3.2. Activation of Carbon Produced of Cavendish Banana Peels Waste

Activation is a process that aims to increase the ability of activated carbon to absorb chemical compounds, gases, or other substances. This process produces a larger surface with more pores to adsorb more compounds. Chemically, carbon is treated with phosphoric acid, sulfuric acid, or alkali metals, which remove organic materials bound to carbon and open pores. In this research, phosphoric acid was used to activate carbon, and characteristics were observed after activation process, as presented in Table 3.

Table 3 The characteristics of activated carbon after activating at different acids and concentrations (Carbonization temperature at 300°C)

Activator	Parameters		
	Moisture Content, %	Ash Content, %	Iodine Adsorption, mg/g
3 % H_3PO_4	21.49	2.81	1866.22
6 % H_3PO_4	19.41	3.56	1884.69
9 % H_3PO_4	18.36	2.95	1885.81
3 % HCl	30.35	4.93	1894.53
6 % HCl	27.06	4.41	1899.91
9 % HCl	22.31	3.39	1914.24

Table 3 shows that the moisture content of activated carbon after acid activation ranged from 19.41 to 30.35%, with the lowest value obtained using the H_3PO_4 as an activator. The decrease in moisture content was attributed to H_3PO_4 (Pujiono et al., 2017), which accelerated the drying process, producing lower moisture content compared to HCl. According to previous research, higher activator concentration would produce lower moisture content of activated carbon (Hendrawan et al., 2017). Phosphoric acid is generally easier to control in reactions due to the lower acidity, minimizing the risk of damage or excessive crushing of activated carbon during activation. Furthermore, it is more suitable for applications requiring larger carbon pores and is less acidic. Based on the results in Table 3, the ash content of activated carbon after acid activation ranged from 2.81 to 4.93%.

The range of activator concentrations did not significantly affect the ash content of activated carbon. However, the H_3PO_4 activator produced a lower value compared to HCl, which was more effective in removing organic materials from activated carbon. The result was consistent with previous research conducted by (Nurrahman et al., 2021), where high acid concentration during activation enhanced the adsorption capacity. Higher acid concentration has also been associated with a greater possibility of a reaction between the activating agent and activated carbon, producing a more significant amount of micropores and mesopores (Tongpoothorn et al., 2011; Moreno-Piraján and Giraldo, 2010). The surface area of activated carbon obtained was increased with higher acid concentration, which enhanced the adsorption capacity. This indicated that high iodine adsorption capacity shows the excellent quality of activated carbon (Maulinda et al., 2015).

Table 4 shows a comparison of adsorption characteristics of activated carbon on iodine from banana peels and other activated carbon sources. These results suggest that activated carbon derived from Cavendish banana peels has a higher iodine adsorption capacity compared to Jatropha curcas and other agricultural wastes such as rice husk, corncob, and wheat straw (Maneechakr and Karnjanakom, 2017; Buasri et al., 2013).

3.3. The Morphology of Activated Carbon Prepared from Cavendish Banana Peels

Figure 2a shows carbon from banana peels after carbonization using a furnace at 300°C for 2 hours. During the carbonization process, the yellow banana peels turned black. Activated carbon morphologies at 1.00 Kx magnifications before and after activation process are shown in Figures 2b and 2c. Specifically, Figure 2b shows a rough and compact surface with irregular shape pores, which is also microporous with vast heterogeneity. After activation process, the morphology changed into porous materials of regular shape and opened pores. Following the carbonization and

acid activation process, tiny pores with a diameter of less than 6 µm are formed, along with an increase in the number and diameter of pores. Additionally, the presence of 9% acidic chloride leads to larger pore size and opening of tinier pores. This shows that acidic chloride can effectively remove hydrocarbon compounds attached to carbon surface after the carbonization process.

Table 4 The iodine adsorbed by activated carbon obtained from different carbon sources

Adsorbent	Qe (mg/g) for I_2	Reference
AC banana peels	1914.24	
ACC	1186.17	(Maneechakr and Karnjanakom, 2017)
CB	307.82	
401	380.01	
402	397.98	
501	580.33	
502	590.56	
AC with soaking HF	300	(Buasri et al., 2013)
AC without soaking HF	290	

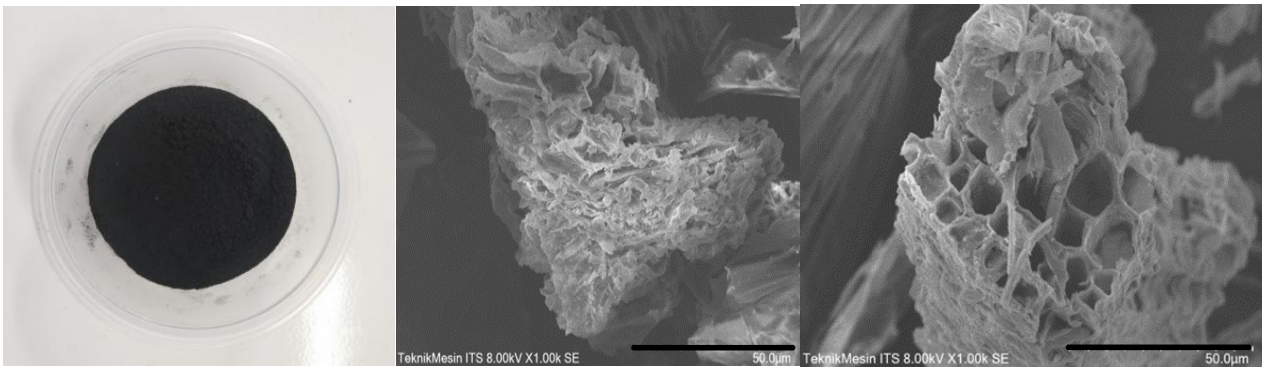

(a) (b) (c)

Figure 2 Producing activated carbon from Cavendish banana: (a) Carbon after carbonization at 300°C, Scanning Electron Microscopy (SEM) with scale bar 50µm of (b) Carbon after carbonization, (c) Carbon after activation

3.4. The FTIR identification of Activated Carbon prepared from Cavendish Banana Peels

Figure 3 shows FTIR spectra of dried banana peels and activated carbon within the 4000-400 cm^{-1} range. Based on the results, the band in the region of 3423 cm^{-1} shows the presence of the stretching vibration of amine (–NH) and O-H functional groups (Al-Tabakha et al., 2021). The band at 2924 cm^{-1} is allocated to aliphatic acid C–H stretching vibrations (El-Din et al., 2018), while 1654 cm^{-1} represents the skeletal aromatic vibrations of C=C in lignin (Gonultas and Candan, 2018), and 1404 cm^{-1} shows –C-H bending. The results of FT-IR analysis on activated carbon show changes in the infrared (IR) absorption spectrum pattern, namely a reduction in intensity at wave numbers from 3423 cm^{-1}, 2924 cm^{-1}, 2372 cm^{-1}, and 1404 cm^{-1}. Subsequently, new absorptions are formed at wave numbers 2848 cm^{-1}, which is the C-H stretching vibration of methyl (CH_3) and methylene (CH_2) groups, with 1265 cm^{-1} representing the C-O functional group. Carbonization and activation processes have also been established for aromatic C=C bonds at wave number 1589 cm^{-1}, showing an increase in aromatic compounds. These compounds are structural components of hexagonal activated carbon, showing the pore structure of activated carbon, as validated by morphological analysis using SEM. Activated carbon produced has an absorption pattern with OH, C-H, C-O, and C=C bond types. The presence of the OH and C-O bonds suggests that activated carbon tends to be polar showing the suitability of activated carbon as an adsorbent for polar compounds (Wibowo et al., 2011).

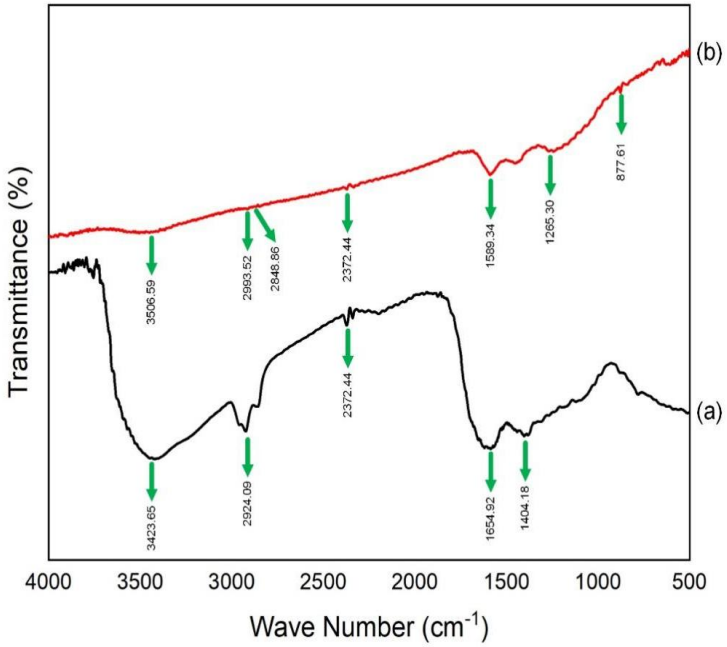

Figure 3 FTIR spectra of (a) dried Banana peels, and (b) activated carbon after carbonization and acid activation

3.5. Brunauer-Emmet-Teller (BET) Analysis

Activated carbon was analysed using BET equipment to determine physicochemical properties after being subjected to carbonization and chemical activation. Based on the results, the BET surface area was found to be 272.84 m^2/g and 421.63 m^2/g aft*er* both processes, respectively. The analysis showed that activated carbon possessed total pore volumes of 0.217 cm^3/g and 0.319 cm^3/g, with average pore diameters of 3.188 nm and 3.024 nm after carbonization and chemical activation (HCl 9%), respectively. The FTIR results showed that the chemical activation caused the loss of organic compounds in activated carbon, leading to an increase in surface area and total pore volume. Activated carbon had an average pore size within the mesoporous range (2–50 nm). Table 5 shows a comparison of the surface area of activated carbon derived from banana peels and other natural materials. The materials were activated through acid impregnation followed by carbonization.

Based on the data presented in Table 5, activated carbon produced from banana peels through the carbonization process and treated with HCl showed superior results compared to solid waste generated during the production of sunflower oil treated with H_2SO_4. This phenomenon could be attributed to the fiber structure of banana peels, which was longer than sunflower oil cake waste. However, activated carbon obtained from bamboo showed improved performance than banana peels through HCl activation. This could be attributed to the compact, long, and sturdy structure of bamboo, which led to the formation of solid pores in activated carbon.

Table 5 Comparison of different adsorbents related to their activated treatments

Raw Materials of Adsorbent	Impregnating Agent	Surface Area S_{BET} (m^2/g)	Reference
Banana peels	HCl	421.63	-
Sunflower oil cake	H_2SO_4	241	(Ratan et al., 2018)
Bamboo	HCl	482	(Mui et al., 2010)
	HNO_3	295	
	H_2SO_4	554	
Carbon	HClO	74-79	(Din et al., 2017)

3.6. Adsorption Performance of Activated Carbon for Ferric Ions Removal

According to the data shown in Figure 4, the process of adsorption could be divided into a fast and a slow stage. During the initial stage (0-45 min), ferric ions were quickly adsorbed onto the available sites on the surface of activated carbon. The adsorption capacity of activated carbon for ferric ions was observed to increase along with adsorption time, reaching a maximum of 1.1015 mg/g after 90 minutes. Subsequently, the number of available adsorption sites on the surface of activated carbon started to decrease, causing the adsorption capacity to gradually reach saturation. During the slow stage of adsorption (45-90 min), the adsorption capacity of ferric ions increased from 0.7794 mg/g to 1.102 mg/g. This showed that the process was time-dependent, showing the need for optimization to achieve the maximum adsorption capacity. (Wang and Xu, 2024).

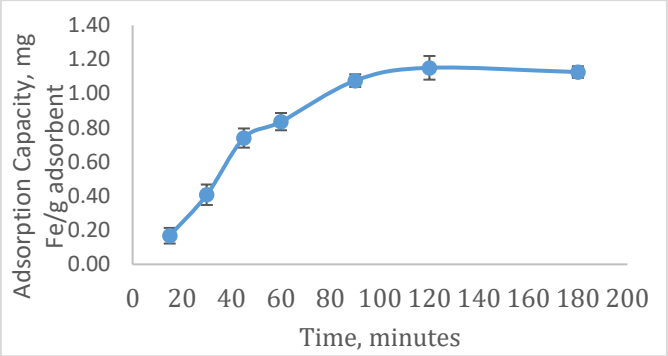

Figure 4 Ferric ions adsorption using activated carbon from Cavendish banana Peels

The initial Fe ions concentration of 2.8 mg/L produced an adsorption capacity of 1.1015 mg Fe/g. Although activated carbon obtained from banana peels could be regenerated four times, the efficiency would reduce by 75% after each regeneration. Based on the results, the Freundlich model's correlation coefficient (R^2) is closer to 1 and has a higher value compared to the Langmuir model. The Freundlich isotherm is based on the assumption that adsorption occurs on sites with non-uniform energy level distribution, rather than on a uniform surface. This shows that adsorption is reversible and not limited to monolayer formation. As presented in Figure 5 and Figure 6, R^2 values suggest that the adsorption of ferric ions in this research is well-suited to the Freundlich model, showing the potential formation of heterolayer ferric ions on the adsorbent surface. This phenomenon can be explained by the surface chemistry of banana peels, which have active functional groups with different intensities and non-uniform distribution.

The presence of these functional groups affects the adsorption power by causing differences in the energy level of the active sites available on the surface (Achak et al., 2009). Moreover, active sites with higher energy levels tend to form heterolayer ferric ions adsorption. This shows that activated carbon's adsorption of ferric ions is mainly dominated by physical adsorption, such as van der Waals force and Cπ – cation interactions. Van der Waals interactions occur between iron ions and activated carbon due to the uneven distribution of electrons and the dipole moment. Metal ions interact with activated carbon through Cπ-Fe^{3+} interactions, facilitating the adsorption onto the surface and pores. Previous research has also shown that activated carbon system is best represented by the Freundlich model, with a capacity of 0.027 mg Fe/g activated carbon (Meisrilestari et al., 2013).

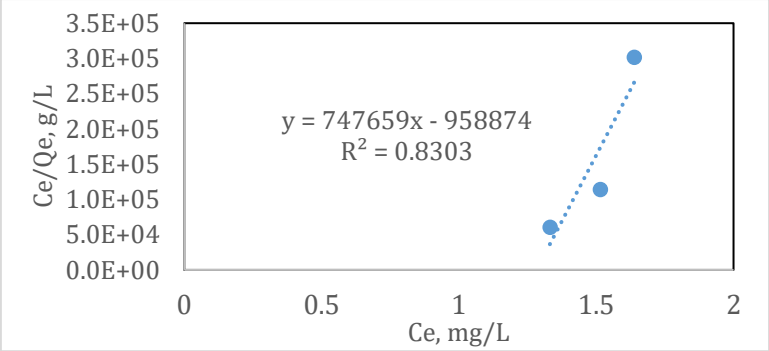

Figure 5 Linear fit of Langmuir isotherm adsorption of ferric ions by activated carbon from Cavendish banana peels

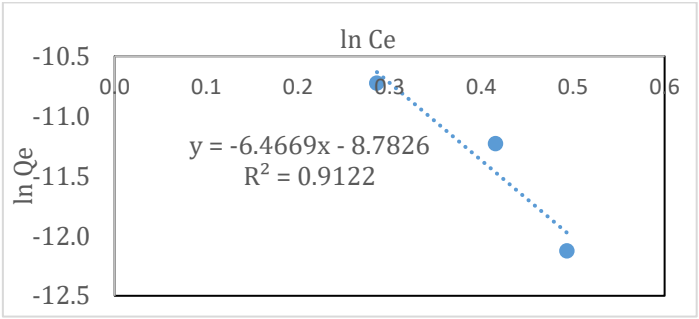

Figure 6 Linear fit of Freundlich isotherm adsorption of ferric ions by activated carbon for Cavendish banana peels

Table 6 shows a comparison of the heavy metal adsorption capabilities of activated carbon sourced from banana peels and other agricultural waste. Based on the data presented, activated carbon obtained from banana peels and betel nut skins has a lower adsorption capacity compared to other forms. This can be due to several factors, including the presence of mesopores in activated carbon obtained from banana peels, which may not be suitable for Fe^{3+} ions. Moreover, the larger pore size of activated carbon allows for easier access to Fe^{3+} ions, entering activated carbon structure. The pH level during the adsorption test can also affect the adsorption capacity of activated carbon.

Table 6 The heavy metal adsorbed by activated carbon obtained from different carbon sources

Adsorbent	Qe (mg/g) for Fe^{3+}	Qe (mg/g) for Fe^{2+}	Qe (mg/g) for $Cr_2O_7^{2+}$	Reference
AC banana peels	1.102			
ACC		5.42	0.72	(Maneechakr and Karnjanakom, 2017)
CB		13.53	0	
401		14.55	0	
402		15.80	0	
501		21.33	0	
502		23	0	
AC Betel nut skin		1.4174		(Herlinawati et al., 2023)

4. Conclusions

In conclusion, this research showed that Cavendish banana peels waste could be used to effectively prepare activated carbon. Based on the results, the suitable conditions to achieve optimum iodine number were 300°C carbonization temperature, 24-hour activation time, and 9%

hydrochloric acid. The adsorption capacity for iodine and ferric ions reached 1914.24 and 1.1015 mg Fe/g activated carbon and fit the Freundlich isotherm model. Although activated carbon obtained from banana peels could be regenerated for approximately four times, the efficiency would reduce by 75% after each regeneration.

Acknowledgements

The author is grateful for the financial support received from the Indonesian Ministry of Research, Technology, and Higher Education through the Fundamental Research Scheme for Higher Education Excellence under contract numbers 077/E5/PG.02.00.PL/2023 and 004/SP2H/PT-L/LL7/2023.

Author Contributions

Restu Kartiko Widi conceived the idea, verified methods, designed experiment, and wrote the manuscript; Puguh Setyopratomo conceived the Idea, verified methods and designed experiment; Priscilla Eveline Danatha, and Verina Dione Nanlohy carried out experiments; Emma Savitri analysed, validated data, wrote and edited the manuscript; all authors discussed results and reviewed the manuscript. All authors have read and agreed to the published version of the manuscript.

Conflict of Interest

The authors declare that there is no conflict of interest regarding the publication of this manuscript. The research was conducted in the absence of any commercial or financial relationships that could be construed as a potential conflict of interest.

References

Achak, M, Hafidi, A, Ouazzani, N, Sayadi, S & Mandi, L 2009, 'Low cost biosorbent "banana peel" for the removal of phenolic compounds from olive mill wastewater: Kinetic and equilibrium studies', *Journal of Hazardous Materials,* vol. 166, no. 1, pp. 117–125, https://doi.org/10.1016/j.jhazmat.2008.11.036

Adekanmi, AT 2021, 'Health hazards of toxic and essential heavy metals from the poultry waste on human and aquatic organisms', In: *Animal Feed Science and Nutrition,* IntechOpen, Rijeka, https://doi.org/10.5772/intechopen.99549

Al-Tabakha, MM, Khan, SA, Ashames, A, Ullah, H, Ullah, K, Murtaza, G & Hassan, N 2021, 'Synthesis, characterization and safety evaluation of sericin-based hydrogels for controlled delivery of acyclovir', *Pharmaceuticals*, vol. 14, No. 3, article 234, https://doi.org/10.3390/ph14030234

Anhwange, B, Ugye, J & Nyiatagher, TD 2009, 'Chemical composition of Musa sepientum (banana) peels', *Electronic Journal of Environment, Agriculture and Food Chemistry*, vol. 8, pp. 437–442

Basheer, AO, Hanafiah, MM, Alsaadi, MA, Al-Douri, Y & Al-Raad, AA 2021, 'Synthesis and optimization of high surface area mesoporous date palm fiber-based nanostructured powder activated carbon for aluminum removal', *Chinese Journal of Chemical Engineering*, vol. 32, pp. 472–484, https://doi.org/10.1016/j.cjche.2020.09.071

Basuki, KT, Fatuzzahroh, M, Ariyanti, D & Saputra, A 2021, 'Adsorption of strontium from an aqueous solution by TiO_2-pillared zeolite', *International Journal of Technology*, vol. 12, pp. 625–634, https://doi.org/10.14716/ijtech.v12i3.4376

Bhushan, B, Nayak, A & Kotnala, S 2021, 'Green synthesis of highly porous activated carbon from jackfruit peel: Effect of operating factors on its physico-chemical characteristics', *Materials Today: Proceedings*, vol. 44, no. 1, pp. 187–191, https://doi.org/10.1016/j.matpr.2020.08.554

Buasri, A, Chaiyut, N, Loryuenyong, V, Phakdeepataraphan, E, Watpathomsub, S & Kunakemakorn, V 2013, 'Synthesis of activated carbon using agricultural wastes from biodiesel production', *International Journal of Materials and Metallurgical Engineering*, vol. 7, no. 1, pp. 106–110

Darmadi, Lubis, MR, Masrura, M, Syahfatra, A & Mahidin 2023, 'Clay and zeolite-clay based monoliths as adsorbents for the Hg(II) removal from the aqueous solutions', *International Journal of Technology*, vol. 14, pp. 129–141, https://doi.org/10.14716/ijtech.v14i1.5134

Dhaneswara, D, Tsania, A, Fatriansyah, JF, Federico, A, Ulfiati, R, Muslih, R & Mastuli, MS 2024, 'Synthesis of mesoporous silica from sugarcane bagasse as adsorbent for colorants using cationic and non-ionic surfactants', *International Journal of Technology*, vol. 15, no. 2, pp. 373-382, https://doi.org/10.14716/ijtech.v15i2.6721

Din, MI, Ashraf, S & Intisar, A 2017, 'Comparative study of different activation treatments for the preparation of activated carbon: A mini-review', *Science Progress*, vol. 100, no. 3, pp. 299-312, https://doi.org/10.3184/003685017X14967570531606

El-Din, GA, Amer, AA, Malsh, G & Hussein, M 2018, 'Study on the use of banana peels for oil spill removal', *Alexandria Engineering Journal*, vol. 57, pp. 2061–2068, https://doi.org/10.1016/j.aej.2017.05.020

ElShafei, GMS, ElSherbiny, IMA, Darwish, AS & Philip, CA 2014, 'Silkworms' feces-based activated carbons as cheap adsorbents for removal of cadmium and methylene blue from aqueous solutions', *Chemical Engineering Research and Design*, vol. 92, no. 3, pp. 461–470, https://doi.org/10.1016/j.cherd.2013.09.004

Falowo, TT, Ejidike, IP, Lajide, L & Clayton, HS 2021, 'Polyphenolic content of Musa acuminata and Musa paradisiaca bracts: Chemical composition, antioxidant and antimicrobial potentials', *Biomedical and Pharmacology Journal*, vol. 14, pp. 1767–1780, https://doi.org/10.13005/bpj/2276

Gonultas, O & Candan, Z 2018, 'Chemical characterization and FTIR spectroscopy of thermally compressed eucalyptus wood panels', *Maderas: Ciencia y Tecnología*, vol. 20, pp. 431–442, https://doi.org/10.4067/S0718-221X2018005031301

Hendrawan, Y, Sutan, SM, Kreative, R, Keteknikan, J, Teknologi, PF, Brawijaya, PU & Malang, JV 2017, 'Pengaruh variasi suhu karbonisasi dan konsentrasi aktivator terhadap karakteristik karbon aktif dari ampas tebu (bagasse) menggunakan activating agent NaCl' (The effect of carbonization temperature variation and activator concentration on the characteristics of activated carbon from sugarcane bagasse using activating agent NaCl), *Jurnal Keteknikan Pertanian Tropis dan Biosistem,* vol. 5, no. 3, pp. 200-207, https://jkptb.ub.ac.id/index.php/jkptb/article/view/420

Herlinawati, H, Sihombing, JL, Kembaren, A, Simatupang, L & Adhani, R 2023, 'Analysis of Fe metal adsorption in industrial wastewater using adsorbents from betel nut skin', *Jurnal Pendidikan Kimia*, vol. 15, no. 1, pp. 35–40, https://doi.org/10.24114/jpkim.v15i1.42478

Jodiawan, J, Chrisdiyanti, DN, Vi'atin, N, Prihastyanti, MNU, Chandra, RD, Heriyanto, H, Siswanti, CA, Hapsari, L & Brotosudarmo, THP 2021, 'Carotenoid analysis from commercial banana cultivars (Musa spp.) in Malang, East Java, Indonesia', *Indonesian Journal of Chemistry*, vol. 21, pp. 690–698, https://doi.org/10.22146/ijc.60865

Kusrini, E, Ayuningtyas, K, Mawarni, DP, Wilson, LD, Sufyan, M, Rahman, A, Prasetyanto, YEA & Usman, A 2021, 'Micro-structured materials for the removal of heavy metals using a natural polymer composite', *International Journal of Technology*, vol. 12, no. 2, pp. 275–286, https://doi.org/10.14716/ijtech.v12i2.4578

Luangkiattikhun, P, Tangsathitkulchai, C & Tangsathitkulchai, M 2008, 'Non-isothermal thermogravimetric analysis of oil-palm solid wastes', *Bioresource Technology*, vol. 99, pp. 986–997, https://doi.org/10.1016/j.biortech.2007.03.001

Maneechakr, P & Karnjanakom, S 2017, 'Adsorption behaviour of Fe(II) and Cr(VI) on activated carbon: Surface chemistry, isotherm, kinetic and thermodynamic studies', *Journal of Chemical Thermodynamics*, vol. 106, pp. 104–112, https://doi.org/10.1016/j.jct.2016.11.021

Maulinda, L, Nasrul, ZA & Sari, DN 2015, 'Pemanfaatan kulit singkong sebagai bahan baku karbon aktif' (Utilization of cassava skin as raw material for activated carbon), *Jurnal Teknologi Kimia Unimal,* vol. 4, no. 2, pp. 11-19

Meisrilestari, Y, Khomaini, R & Wijayanti, H 2013, 'Pembuatan arang aktif dari cangkang kelapa sawit dengan aktivasi secara fisika, kimia dan fisika-kimia' (Production of activated charcoal from palm shells by physical, chemical and physical-chemical activation), *Konversi*, vol. 2, no. 1, pp. 45-50, https://doi.org/10.20527/k.v2i1.136

Mistar, EM, Alfatah, T & Supardan, MD 2020, 'Synthesis and characterization of activated carbon from Bambusa vulgaris striata using two-step KOH activation', *Journal of Materials Research and Technology*, vol. 9, no. 3, pp. 6278–6286, https://doi.org/10.1016/j.jmrt.2020.03.041

Moreno-Piraján, JC & Giraldo, L 2010, 'Study of activated carbons by pyrolysis of cassava peel in the presence of chloride zinc', *Journal of Analytical and Applied Pyrolysis*, vol. 87, pp. 288–290, https://doi.org/10.1016/j.jaap.2009.12.003

Mui, ELK, Cheung, WH, Valix, M & Mckay, G 2010, 'Dye adsorption onto char from bamboo', *Journal of Hazardous Materials*, vol. 177, no. 1–3, pp. 1001–1005, https://doi.org/10.1016/j.jhazmat.2010.01.018

Nurrahman, A, Permana, E, Gusti, DR & Lestari, I 2021, 'Pengaruh konsentrasi aktivator terhadap kualitas karbon aktif dari batubara lignit'(Effect of activator concentration on the quality of activated carbon from lignite coal), *Jurnal Daur Lingkungan*, vol. 4, no. 2, pp. 44-53, https://doi.org/10.33087/daurling.v4i2.86

Peláez-Cid, AA, Romero-Hernández, V, Herrera-González, AM, Bautista-Hernández, A & Coreño-Alonso, O 2020, 'Synthesis of activated carbons from black sapote seeds, characterization and application in the elimination of heavy metals and textile dyes', *Chinese Journal of Chemical Engineering*, vol. 28, no. 2, pp. 613–623, https://doi.org/10.1016/j.cjche.2019.04.021

Prakash, MO, Raghavendra, G, Ojha, S, Panchal, M & Kumar, D 2021, 'Investigation of tribological properties of biomass developed porous nano activated carbon composites', *Wear*, vol. 466–467, article 203523, https://doi.org/10.1016/j.wear.2020.203523

Pujiono, EF & Mulyati, A 2017, 'Potential of activated carbon produced from agriculture waste for water treatment material', *Jurnal Wiyata,* vol. 1, no. 1, pp. 37-45, http://dx.doi.org/10.56710/wiyata.v4i1.94

Ratan, JK, Kaur, M & Adiraju, B 2018, 'Synthesis of activated carbon from agricultural waste using a simple method: Characterization, parametric and isotherms study', *Materials Today: Proceedings*, vol. 5, no. 2, pp. 3334–3345, https://doi.org/10.1016/j.matpr.2017.11.576

Sanchez-Sanchez, A, Izquierdo, MT, Mathieu, S, Medjahdi, G, Fierro, V & Celzard, A 2020, 'Activated carbon xerogels derived from phenolic oil: Basic catalysis synthesis and electrochemical performances', *Fuel Processing Technology*, vol. 205, article 106427, https://doi.org/10.1016/j.fuproc.2020.106427

Sudaryanto, Y, Hartono, SB, Irawaty, W, Hindarso, H & Ismadji, S 2006, 'High surface area activated carbon prepared from cassava peel by chemical activation', *Bioresource Technology*, vol. 97, no. 5, pp. 734–739, https://doi.org/10.1016/j.biortech.2005.04.029

Timotius, D, Kusumastuti, Y, Omar, R, Harun, R, Kamal, SMM, Jenie, SNA & Petrus, HTBM 2022, 'The study of methylene blue loading into chitosan-graft-maleic sponges', *International Journal of Technology*, vol. 13, no. 8, pp. 1796-1805, https://doi.org/10.14716/ijtech.v13i8.6133

Tongpoothorn, W, Sriuttha, M, Homchan, P, Chanthai, S & Ruangviriyachai, C 2011, 'Preparation of activated carbon derived from Jatropha curcas fruit shell by simple thermo-chemical activation and characterization of their physico-chemical properties', *Chemical Engineering Research and Design*, vol. 89, no. 3, pp. 335–340, https://doi.org/10.1016/j.cherd.2010.06.012

Tripathy, A, Mohanty, S, Nayak, SK & Ramadoss, A 2021, 'Renewable banana-peel-derived activated carbon as an inexpensive and efficient electrode material showing fascinating supercapacitive performance', *Journal of Environmental Chemical Engineering*, vol. 9, No. 6, article 106398, https://doi.org/10.1016/j.jece.2021.106398

Wang, K & Xu, S 2024, 'Preparation of high specific surface area activated carbon from petroleum coke by KOH activation in a rotary kiln', *Processes*, vol. 12, no. 2, article 241, https://doi.org/10.3390/pr12020241

Wibowo, S, Syafi, W & Pari, G 2011, 'Karakterisasi permukaan arang aktif tempurung biji nyamplung (surface analysis of activated charcoal from nyamplung seed shells)', *Makara,* vol. 15, no. 1, pp. 17-24

Wikantika, K, Ghazali, MF, Dwivany, FM, Novianti, C, Yayusman, LF & Sutanto, A 2022, 'Integrated studies of banana on remote sensing, biogeography, and biodiversity: An Indonesian perspective', *Diversity*, vol. 14, no. 4, article 277, https://doi.org/10.3390/d14040277

Yagmur, HK & Kaya, I 2021, 'Synthesis and characterization of magnetic ZnCl2-activated carbon produced from coconut shell for the adsorption of methylene blue', *Journal of Molecular Structure*, vol. 1232, article 130071, https://doi.org/10.1016/j.molstruc.2021.130071

Yanti, I, Sationo, PP, Winata, WF, Anugrahwati, M, Anas, AK & Swasono, YA 2023, 'Effectiveness of activated carbon magnetic composite from banana peel (Musa acuminata) for recovering iron metal ions', *Case Studies in Chemical and Environmental Engineering*, vol. 8, article 100378, https://doi.org/10.1016/j.cscee.2023.100378

Yu, F, Zhu, X, Jin, W, Fan, J, Clark, JH & Zhang, S 2020, 'Optimized synthesis of granular fuel and granular activated carbon from sawdust hydrochar without binder', *Journal of Cleaner Production*, vol. 276, article 122711, https://doi.org/10.1016/j.jclepro.2020.122711

Zhang, D, He, C, Zhao, J, Wang, J & Li, K 2019, 'Facile synthesis of hierarchical mesopore-rich activated carbon with excellent capacitive performance', *Journal of Colloid and Interface Science*, vol. 546, pp. 101–112, https://doi.org/10.1016/j.jcis.2019.03.059

Zhou, P, Li, X, Zhou, J, Peng, Z, Shen, L & Li, W 2023, 'Insights of the adsorption mechanism of methylene blue on biochar from phytoextraction residues of Citrus aurantium L.: Adsorption model and DFT calculations', *Journal of Environmental Chemical Engineering*, vol. 11, no. 5, article 110496 https://doi.org/10.1016/j.jece.2023.110496